An Enhanced Technique for Reactor Coolant Pump Abnormality Monitoring Using Continuous Wavelet Transform Based Sparse Code Shrinkage De-noising Algorithm

M. Boufenar, S.Rechak, M.Rezig

International Atomic Energy Agency, Vienna International Centre P.O. Box 100, A-1400 Vienna, Austria

boufmed@hotmail.com

1. Background and Goal of the present work.

Detection of the weak signature of degradation of the Reactor Coolant Pump (RCP) at early stage gives more time for maintenance reaction, safety decision-making and also provides economic benefits. An integrated and improved method to detect and identify abnormality using continuous wavelet transform based sparse code shrinkage de-noising algorithm is suggested in this work. For RCP roller bearings, periodic impulses indicate the occurrence of faults in the components. However, it is difficult to detect the impulses because they are rather weak and are often immersed in heavy noise. Existing wavelet threshold de-noising methods do not work well because they use orthogonal wavelets, which do not match the impulse very well and do not utilize prior information on the impulse. Therefore, in order to suppress any undesired information and highlight the features of interest, a new method for wavelet threshold de-noising is proposed in this paper. It employs an adapted Morlet wavelet as the basic wavelet for matching the impulse and also uses the Maximum Likelihood Estimation (MLE) for thresholding by utilizing prior information on the probability density function (pdf) of the impulse. By using MLE de-noising method, the inspected signal is analyzed in a more exact way even with a very low signal-to-noise ratio.

1.1. Review of wavelet Transform

The wavelet transform of a finite energy signal $x(t)$ with the analyzing wavelet $\psi(t)$ is the convolution of with a scaled and conjugated wavelet. Let $\psi_{a,b}(t)$ the daughter wavelets of the mother wavelet $\psi(t)$, which is derived by varying both the scale factor *a* and the shifting parameter *b* :

$$\psi_{a,b}(t) = \frac{1}{\sqrt{a}}\psi\left(\frac{t-b}{a}\right) \qquad (1)$$

The wavelet transform is defined as:

$$W_{\psi}(a,b) = \langle x(t), \psi_{a,b}(t)\rangle = \frac{1}{\sqrt{a}}\int_{-\infty}^{\infty} x(t)\psi^{*}{}_{a,b}(t)dt \qquad (2)$$

The parameters of translation *a* and dilation *b*, may be continuous or discrete, the asterisk stands for complex conjugate. The factor $1/\sqrt{a}$ is used to ensure energy preservation. Eq. (2) indicates that the wavelet analysis is a time-frequency analysis, or a time-scaled analysis of a signal through dilation and translation.

1.2. Mechanical impulse modelling

The system subjected to an impact load may be formulated as a single degree of freedom system which has the form of:

$$M\frac{d^2x}{dt^2} + C\frac{dx}{dt} + Kx = F\delta(t) \qquad \text{with} \qquad \delta(t) = \begin{cases} 1, & t = b \\ 0, & otherwise \end{cases} \qquad (3)$$

When the initial displacement and velocity of the system are zero, the solution for Eq. (3) can be rewritten as:

$$x(t) = Ae^{-\zeta\omega_n t}cos(\omega_d t) \qquad A = \frac{F}{M\omega_d} \qquad (6)$$

2. Choice of the analyzing wavelet

Eq. (6) indicates that the impulsive feature, which is caused by external impact load, is characterized by an oscillation with decaying amplitude. So according to the matching mechanism of wavelet transform, Morlet wavelet could be a more suitable wavelet function for extracting such types of features because Morlet wavelet has a more similar shape to the impulsive feature. Morlet wavelet is derivative of a Gaussian function, so these wavelets have Gaussian window in frequency domain. In time domain, the Morlet wavelet can be expressed as :

$$\psi(t) = exp^{-\beta^2 t^2/2}\left(exp^{j\omega_0 t} - exp^{-(\omega_0)^2/2}\right) \qquad (7)$$

It is shown that the function decays exponentially on both sides. The wavelet transform using Morlet wavelet as analysis function can take the following form:

$$W_{\psi}(a,b) = \frac{\sqrt{a}}{\sqrt{2\pi}}\int_{-\infty}^{+\infty} X(\omega)\left(exp^{-(a\omega-\omega_0)^2/2\beta^2} - exp^{-(a^2\omega^2+\omega_0{}^2)/2\beta^2}\right)e^{j\omega b}d\omega \qquad (8)$$

It is obvious from Eq. (7) that the shape of the basic wavelet is controlled by parameter β. When β tends to be infinite, the Morlet wavelet becomes a Dirac function with the finest time resolution. With β tending to be 0, the Morlet wavelet becomes a cosine function which has the finest frequency resolution. Therefore, there is always an optimal β with the best time-frequency resolution for a certain signal localized in the time-frequency plane. An approach to find the appropriate parameters that can construct an optimal wavelet transform is proposed in the next section. This modified Morlet wavelet function offers a better compromise in terms of localisation, in both time and frequency for a signal, than the traditionally Morlet wavelet function.

3. Optimal Morlet wavelet for impulse detection

The sparseness of wavelet coefficients is often used as the rule for evaluating the efficiency of wavelet transforms. The wavelet corresponding to the fewest and dominant wavelet transformation coefficients of a signal is ideal. Therefore, a variety of sparseness measurement criteria are proposed by researchers. Shannon entropy is one of the well-adopted sparseness criterion. Thereby, wavelet transform coefficients with minimal Shannon entropy can be treated as the sparsest result. Therefore, the corresponding shape factor β can be adopted as the optimal result. Shannon entropy is defined as:

$$E_n = -\sum_i d_i * \log d_i \qquad \sum_{i=1}^{n} d_i = 1 \qquad \text{and} \qquad d_i = \frac{c_i}{\sum c_j} \qquad (9)$$

4. Sparse code shrinkage threshold using the optimal Morlet wavelet transform

The basic idea behind wavelet thresholding is that the energy of the signal to be identified will concentrate on a few wavelet coefficients while the energy of noise will spread throughout all wavelet coefficients. In view of this, Hyvärinen has proposed a so-called sparse code shrinkage method 'SCS' to estimate non-Gaussian data under noisy conditions. It is based on the MLE principle and is successfully used for image de-noising. It demands that the non-Gaussian variable follow a **sparse distribution**. The pdf of a sparse distribution is characterized with a spike at point zero. To represent a sparse distribution, Hyvärinen proposes the following function form:

$$p(s) = \frac{1}{2d}\frac{(\alpha+2)[\alpha(\alpha+1)/2]^{(\alpha/2+1)}}{\left[\sqrt{\alpha(\alpha+1)/2} + |s/d|\right]^{(\alpha+3)}} \qquad (10)$$

For an impulse whose pdf can be represented by Eq. 10, Hyvärinen proposes the following thresholding rule:

$$g(u) = \text{sign}(u)\max\left(0, \frac{|u| - ad}{2} + \frac{1}{2}\sqrt{(|u| + ad)^2 - 4\sigma^2(\alpha+3)}\right) \qquad (11)$$

The reconstruction results from shrunken wavelet coefficients using the thresholding rule given in Eq. 11 represent an approximation to the impulse.

5. Simulation study

The impulses generated by damaged mechanical components often exhibit the shapes shown in Fig.1.a.

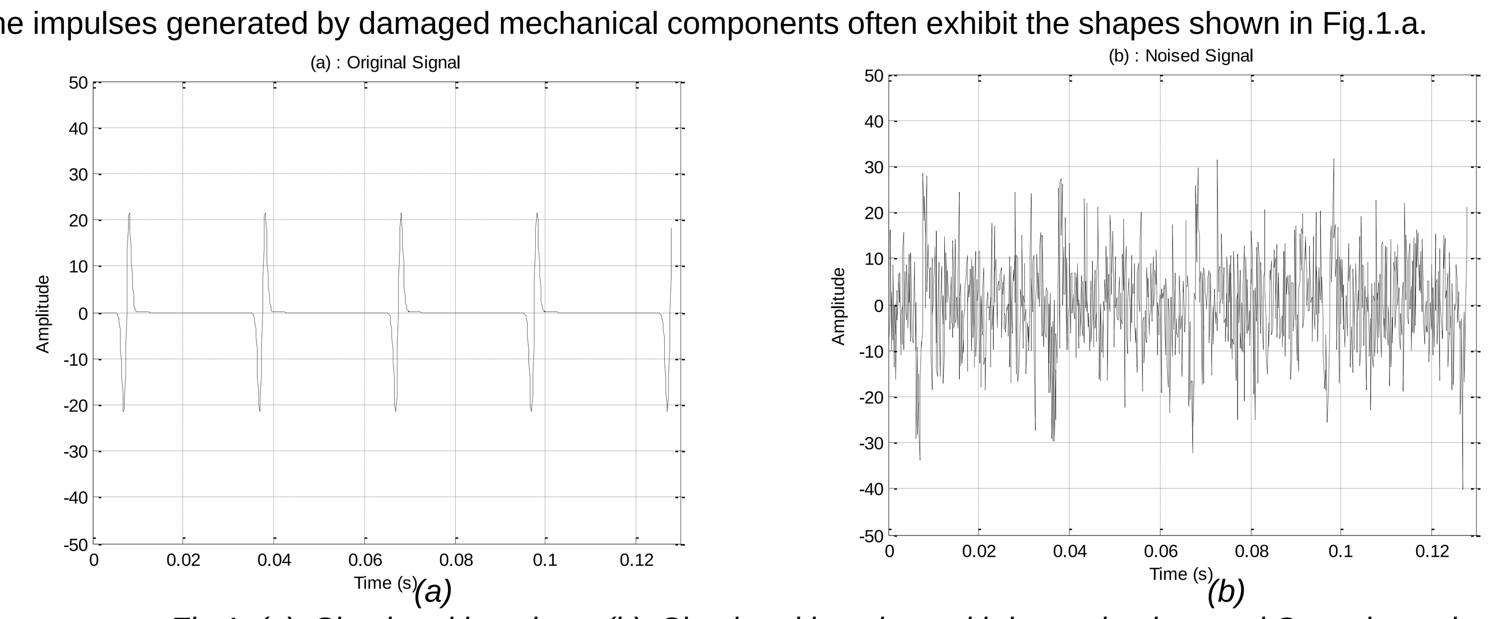

Fig.1. (a): Simulated impulses, (b): Simulated impulses with heavy background Gaussian noise

The signal shown in Fig.1.b is used to test the effectiveness of the proposed method to extract weak periodical impulses from the vibration signals with heavy background noise. The optimal Morlet wavelet is constructed based on the optimization algorithm. The optimal parameter is found as: β = 0.7.

Then, the SCS method is employed to further remove the noise and isolate the impulses. The extracted impulses are presented in Fig.2.a, from which it is observed that all the impulses immersed in noise are picked out.

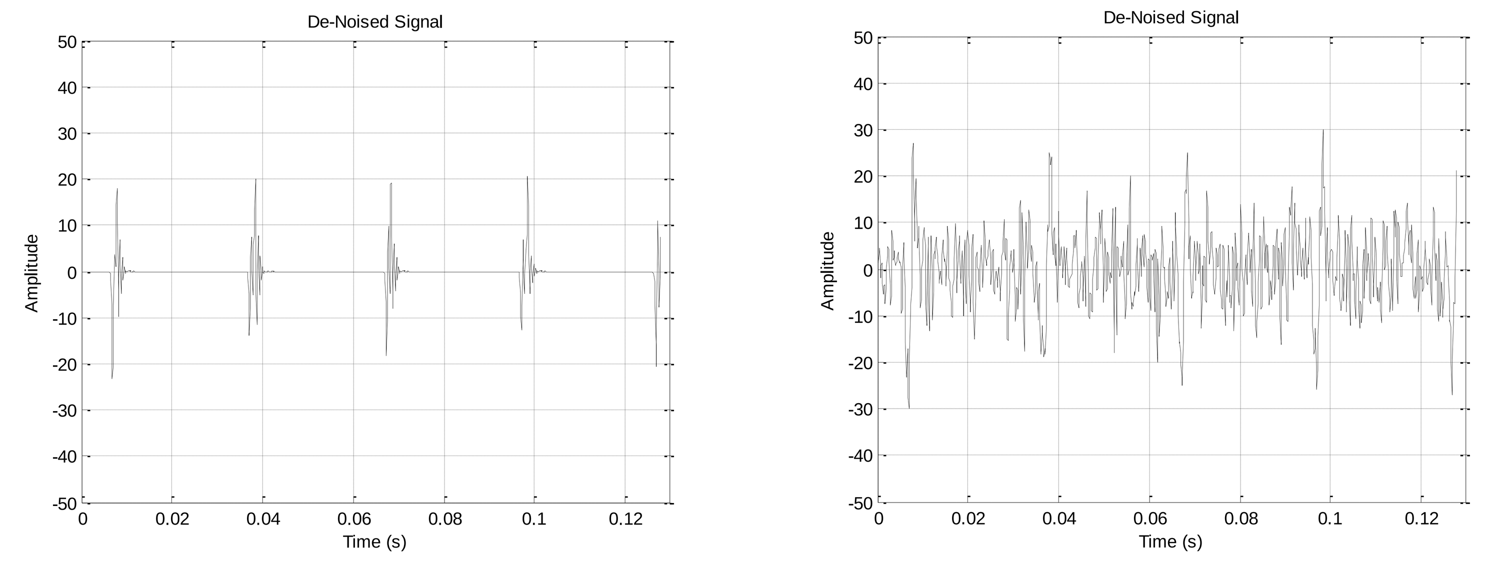

(a) (b)

Fig.2. (a): Result by MLE thresholding, (b): Result by Donoho's soft-thresholding

To further prove the superiority of the proposed method, we also processed the simulation signal using Donoho's 'soft-thresholding de-noising'. Its de-noising result is shown in Fig.2.b. Though several true impulses are extracted, a lot of fake impulses also exist, which would affect the recognition of true impulses.

6. Experimental results

To investigate the effectiveness of SCS de-noising method a series of vibration signals collected from a test rig and from a real machine which is the hydraulic pump of NUR Reactor primary cooling loop system as shown in figures Fig.3 and Fig.4 were analyzed for detecting faults. Vibration signals are collected from accelerometer mounted on the bearing housing.

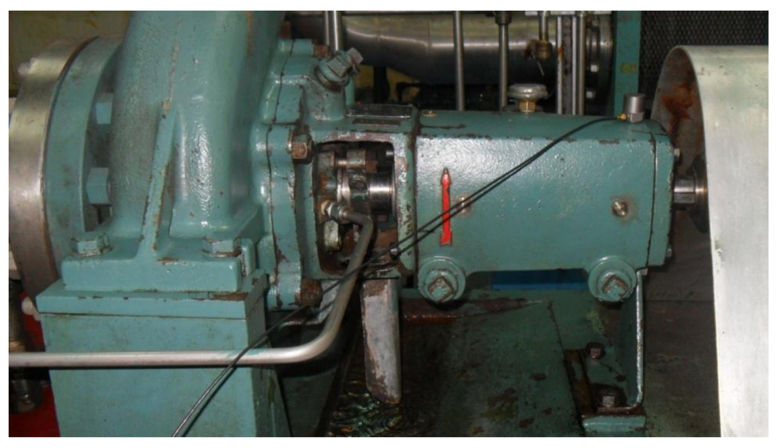

Fig.3. Photograph of the test rig. *Fig.4. NUR Reactor Tested Hydraulic Pump*

A radial acceleration signal was picked up from the top of the tested bearing casing by a B&K 4371 transducer. Afterward, the signal is amplified and band-pass filtered by a B&K charge amplifier into the frequency range from 0.2 Hz to 20 kHz and recorded on the dual channel frequency analyzer B&K 2133. Acquisitions were transferred to the PC where Matlab programs were implemented to execute signal analyses and wavelet transforms calculations. Based on the geometric parameters and the rotational speed of ball bearings, fault characteristic frequencies of bearings are estimated and listed in the following Table 1.

Bearing type	(Test rig bearing) $SNR\ 1205$	(RCP bearing 1) $SKF\ 6309$	(RCP bearing 2) $SKF\ 7309$
Rotating speed (tr/min)	2968	2968	2986
Number of rolling elements	$N = 12$	$N = 8$	$N = 12$
Rotating frequency	$f_r = 49.77\ Hz$	$f_r = 49.47\ Hz$	$f_r = 49.47\ Hz$
Ball Passing Frequency Inner Race - BPFI	$f_i = 353.99\ Hz$ $P_i = 0.0028\ sec$	$f_i = 245.52\ Hz$	$f_i = 352.31\ Hz$
Ball passing Frequency Outer Race - BPFO	$\boldsymbol{f_e = 243.16\ Hz}$ $\boldsymbol{P_e = 0.0041\ sec}$	$f_e = 151.21\ Hz$	$f_e = 241.29\ Hz$

Table 1. Characteristics of the tested bearings

Time and spectral amplitude representing the effect of the crossing of the balls over artificial spall in the test rig bearing is presented in Fig.5.

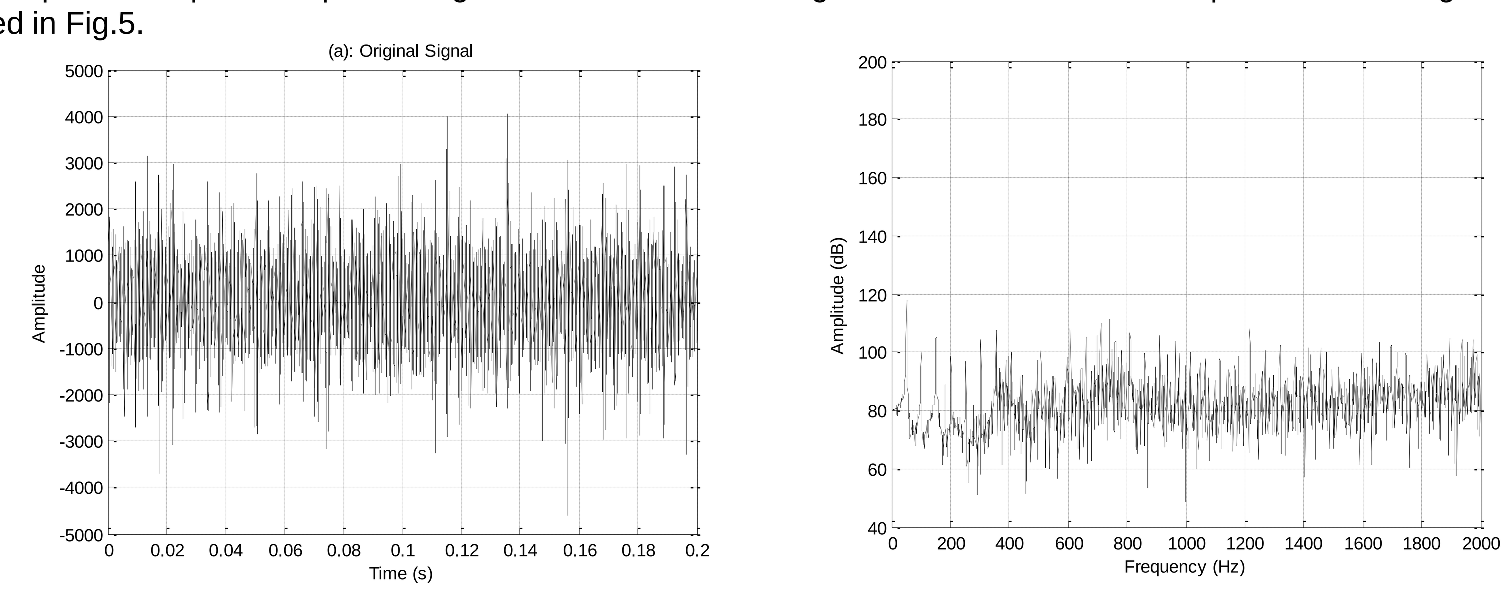

Fig.5. Vibration signal of the tested bearing and its Power spectrum

On the grounds of these observations, it appears clear that the effectiveness of the spectral analysis for the bearing diagnostics proves inadequate to operate correct monitoring. The bearing faults cannot be diagnosed with certainty since spectra provide peaks, located at the fault characteristic frequencies, whose amplitudes are comparable to the corresponding ones related to the bearing in sound condition. Noise prevails over the effect of periodic impulses. However, through the inverse wavelet transform of the thresholded modulus, the reconstructed signal after de-noising by SCS method on the test rig bearing signal is shown in Fig.8.a. Distinct evenly spaced impulses can be observed from the reconstructed signal.

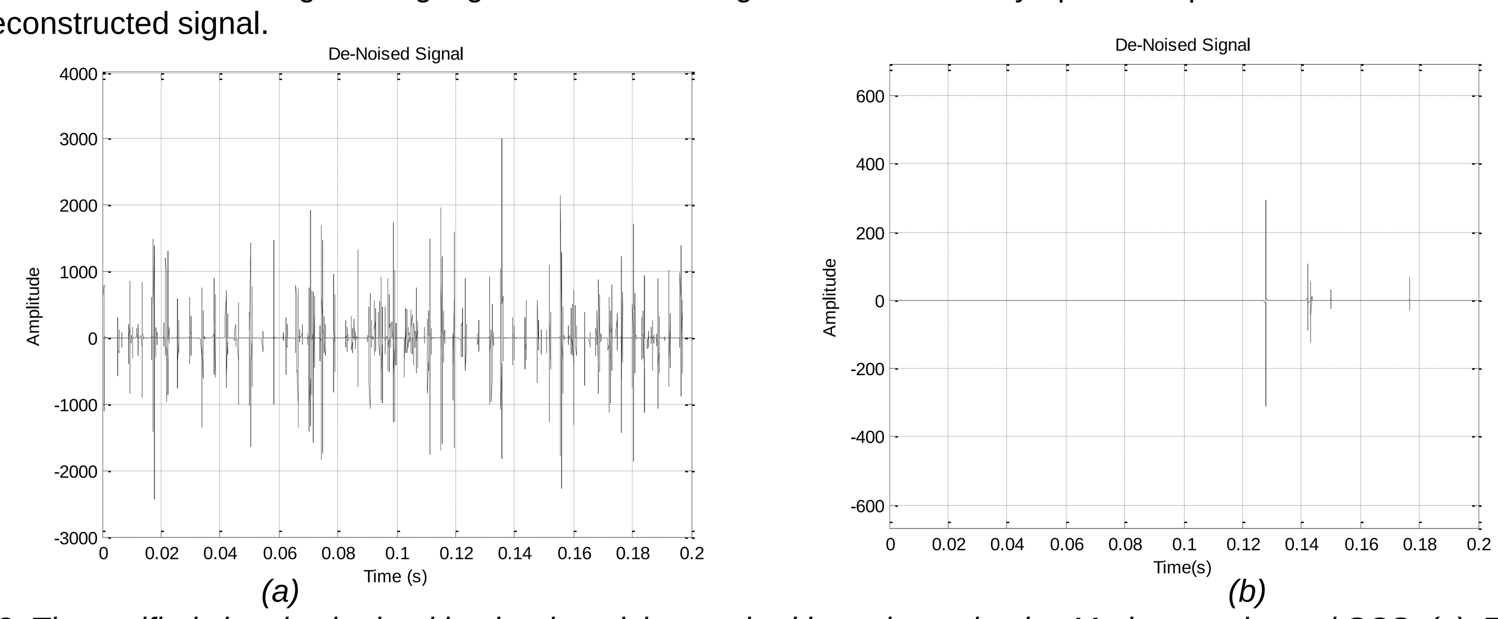

Fig.8. The purified signals obtained by the de-noising method based on adaptive Morlet wavelet and SCS; (a): Test rig bearing signal, (b): RCP bearing signal

The measured distance between two successive impulse peaks of the presented diagrams represents the characteristic defect period, i.e. the inverse of the characteristic frequency. Quasi-periodic intervals equal to 4.1 ms can be found in the figure. These quasi-periodic intervals are equivalent to the inverse of the ball-passing frequency outer-race (BPFO) which is 141 Hz as listed in Table 1. Hence, it can be concluded that the impulses are caused by the outer-race defect. Finally, it is worthwhile to observe from Fig.8.a, that only defect-induced impulse clusters are retained in the reconstructed signal. This indicates the effectiveness of the proposed algorithm in cancelling out the environmental noise even with small defect.

Thereby, the result of SCS de-noising method on RCP bearing signal is plotted in the Fig.8.b. One can observe on reconstructed signal using SCS de-noising method some random peaks without fixed periodicity, which are not related to faulty impulses. It can be concluded now that the reconstructed signal shown in Fig.8.b is the characterised signal pattern of the bearing without raceway defects on bearings. **In view of that, by considering the results obtained, the proposed algorithm shows a great promise in highlighting the defect-induced impact in the vibration signals for bearing fault diagnosis**.

7. Conclusion

The wavelet de-noising method proposed in this paper not only employs the adaptive Morlet wavelet based beta-optimization, as the basic wavelet, but also utilizes prior information on the pdf of the signals to be identified. The new adaptive SCS thresholding rule is effective at extracting the impulsive features buried in the noisy signals even when the SNR is very low. In applications, the SCS thresholding method can be used directly to detect impulses, because the pdf of any impulse signal is always very sparse. such results helps the machine operators not only in detecting the existence of faults on bearing at its initial stage, but also in identifying the causes of faults by using the information of the time intervals which is provided by reconstructed signal.

Poster Ref. Number: B18
International Conference on Research Reactors: Safe Management & Effective Utilization, Rabat, Morocco; 14-18 November 2011